JOURNAL OF MATHEMATICAL PHYSICS **46**, 032106 (2005)

Control of finite-dimensional quantum systems: Application to a spin-$\frac{1}{2}$ particle coupled with a finite quantum harmonic oscillator

C. Rangan
Department of Physics, University of Windsor, Ontario, Canada N9B 3P4

A. M. Bloch
Department of Mathematics, The University of Michigan, Ann Arbor, Michigan 48109-1109

(Received 3 August 2004; accepted 21 November 2004; published online 9 February 2005)

In this paper, we consider the problem of the controllability of a finite-dimensional quantum system in both the Schrödinger and interaction pictures. Introducing a Quantum Transfer Graph, we elucidate the role of Lie algebra rank conditions and the complex nature of the control matrices. We analyze the example of a sequentially coupled N-level system: a spin-$\frac{1}{2}$ particle coupled to a finite quantum harmonic oscillator. This models an important physical paradigm of quantum computers—the trapped ion. We describe the control of the finite model obtained, under the right conditions, from the original infinite-dimensional system. © *2005 American Institute of Physics.* [DOI: 10.1063/1.1852701]

I. INTRODUCTION

The control and controllability of finite-dimensional quantum systems are of topical interest to the chemical dynamics, coherent control and quantum computing communities.[1–9] Indeed, several methods of proving controllability of quantum systems[3,4,10–13] have been developed from corresponding techniques used in the control of finite-dimensional classical systems. In these treatments, specifically in the graphical methods, the role of the drift (or field-free) Hamiltonian is not obvious. In quantum mechanics, it is fairly standard to use an interaction picture, where the drift term does not appear explicitly in the Schrödinger equation. In these cases, the presence of only one matrix, namely the control matrix in the interaction picture, makes it not amenable to use of the rigorous Lie algebraic method[11] to determine controllability.

In this paper, we present fresh insights into the controllability and control of quantum systems both in the Schrödinger and interaction pictures. We propose a new graphical method—the Quantum Transfer Graph—that will explicitly demonstrate both the roles of the drift and control matrices, and also the importance of considering the control matrix as one with complex entries. Then we analyze a very interesting example of a sequentially coupled N-level system: a spin-$\frac{1}{2}$ particle coupled with a quantum harmonic oscillator. This models an important physical paradigm of quantum computers—the trapped ion. The analysis in this paper expands on our earlier work on the trapped-ion problem (Ref. 17) and illustrates the key role played by the Quantum Transfer Graph in understanding the complex matrices that describe the interactions between the field and the ion. To our knowledge this is the only example of a quantum control problem where the interaction matrices are complex. Our general analysis of a sequentially connected system can also be extended to understanding the control of N-level chain systems used in adiabatic schemes such as STIRAP,[14] as well as the control of transitions between sequentially connected Zeeman states.

II. SCHRÖDINGER PICTURE

The Schrödinger equation for a particle in a static and dynamic potential (in atomic units, wherein $e=m=\hbar=1$) is written as

$$\imath|\dot{\Psi}\rangle = (H_0 + H_I)|\Psi\rangle. \tag{1}$$

Here, H_0 is the Hamiltonian of the particle in the static potential, with a finite number (N) of eigenvalues E_n corresponding to the eigenvectors ϕ_n. The interaction with the time-dependent potential is given by the control Hamiltonian H_I, which includes the time dependence. In general, we consider problems where the time dependence is separable and linear, for example, $H_I = \sum_i u_i(t) * \mu_i$. Here the operator μ_i represents the transition couplings between the various eigenstates of H_0 due to the time-dependent field $u_i(t)$. Unitarity demands that H_0 and H_I be Hermitian. The eigenvalues of H_0 are therefore real. In the control literature, the Schrödinger equation is written equivalently as

$$\dot{X} = \left(A + \sum_i u_i(t) B_i\right) X. \tag{2}$$

In vector representation, X is the state vector, A is the drift matrix, B_i are the control matrices and $u_i(t)$ are controls, generally chosen to be piecewise smooth. In the eigenbasis of H_0, A is $-\imath$ times a real matrix with only diagonal terms. Each matrix B_i is skew-Hermitian. It can, in general, be written as a sum of a $\imath$ times a real symmetric matrix and a skew-symmetric matrix, $B_i = \imath * B_i^S + B_i^K$. More generally, $A, B_i \in \mathfrak{su}(N)$. In most quantum applications considered up to this point[2,4,15] the matrix elements of the B_i are of the form $\imath$ times a symmetric matrix. Consider a special case, where the eigenstates of H_0 are sequentially coupled by control fields $u_i(t)$. It is well known[3,9,11] that a sufficient condition for controllability is that the dimension of the span of the Lie algebra generated by A and the B_i be equal to the dimension of $\mathfrak{su}(n)$. Rather than take the specific values for the matrix elements of the control matrices, B_i, it will be instructive to consider its general structure—a skew-Hermitian, tridiagonal matrix with zero diagonal elements. In the case where B is of the form $\imath$ times a symmetric matrix, this matrix can be decomposed into $N-1$ matrices—simple roots of the Lie algebra $\mathfrak{su}(n)$, as shown below. These matrices represent the nearest-neighbor couplings. We want to elucidate how these nearest-neighbor couplings generate the Lie algebra. Note that we do not have control over each individual coupling. Nevertheless, one can see how decomposing the control matrix into the simple roots is a powerful way to examine the controllability properties of the system.

Using standard notation for a basis of $\mathfrak{su}(N)$, let $e_{i,j}$ denote the matrix with unit ij entry and zeros elsewhere. Define $x_{i,j} = e_{i,j} - e_{j,i}$ and $y_{i,j} = \imath(e_{i,j} + e_{j,i})$. B is decomposed into the $\imath$-times-symmetric roots

$$S_1 = y_{1,2} = \imath \begin{pmatrix} 0 & 1 & 0 & 0 & 0 & 0 & \cdots \\ 1 & 0 & 0 & 0 & 0 & 0 & \cdots \\ 0 & 0 & 0 & 0 & 0 & 0 & \cdots \\ 0 & 0 & 0 & 0 & 0 & 0 & \cdots \\ 0 & 0 & 0 & 0 & 0 & 0 & \cdots \\ 0 & 0 & 0 & 0 & 0 & 0 & \cdots \\ \vdots & \vdots & \vdots & \vdots & \vdots & \vdots & \ddots \end{pmatrix}, \tag{3}$$

$$S_2 = y_{2,3}, \tag{4}$$

$$S_3 = y_{3,4}, \tag{5}$$

$$\cdots. \tag{6}$$

The Lie bracket of these roots with each other give the $N-2$ skew-symmetric matrices that represent next-nearest-neighbor coupling as shown below. These matrices form a closed Lie algebra with the matrices from which they were formed, for example, S_1, S_2 and their commutator

$K_N=[S_1,S_2]$ form a Lie subalgebra, similarly for S_2, S_3 and their commutator K_{N+1}, and so on. This generation of alternate symmetric and skew-symmetric elements of the algebra has been observed earlier,[3,13]

$$[S_1,S_2]=x_{1,3}\equiv K_N, \tag{7}$$

$$K_{N+1}=x_{2,4}, \tag{8}$$

$$\cdots. \tag{9}$$

Similarly,

$$[x_{1,3},x_{2,4}]=y_{1,4}\equiv S_{2N-1}. \tag{10}$$

Carrying on in a similar fashion through the matrix that represents the coupling between the first and Nth state (here N is assumed even),

$$S_{N(N-1)/2}=y_{1,N}. \tag{11}$$

It can be shown that the number of linearly independent commutators formed by this set of matrices is $N(N-1)/2$. Thus, the roots of the control Hamiltonian can be used to produce $N(N-1)/2$ independent elements of the algebra.

An interesting observation can be made if the control matrices B_i representing the nearest-neighbor couplings are all skew-symmetric. The Lie algebra generated by these matrices consists of the skew-symmetric matrices, i.e., the symmetric matrices S_n are not generated. These matrices also number $N(N-1)/2$. This is the set of generators for the rotation group $O(N)$, each pairwise coupling representing an independent rotation in N-dimensions.[16]

Thus, if the eigenstates are sequentially connected by the transition matrix elements (usually real), then the Lie algebra generated by the roots of the control terms alone span a space of $N(N-1)/2$. If the drift matrix is strongly regular,[12] it can be decomposed into N linearly independent traceless diagonal matrices $h_i=e_{i,i}-e_{i+1,i+1}$. The Lie brackets formed by the drift matrix and the $N(N-1)/2$ matrices computed above yield another $N(N-1)/2$ matrices of the opposite symmetry. For example, $[A,S_1]$ gives K_1, etc. Thus the total number of linearly independent matrices are $2*N(N-1)/2+N=N^2$, which is sufficient to show controllability.

III. QUANTUM TRANSFER GRAPHS

Graphical methods used to analyze controllability of quantum systems[4,17] are drawn from similar techniques used in the controllability analysis of classical systems.[12] These methods are very elegant. However, they do not bring out two features intrinsic to the controllability of quantum systems—the special role of the drift matrix, and the intrinsically skew-Hermitian nature of the control matrices. To address these issues, we propose that transfer graphs representing the control of quantum systems should be drawn with each eigenstate represented by a double node, representing the real and imaginary parts of the complex wave function. The transition matrix elements are represented by edges of the graph. However, a real matrix element will couple the real part of one state with the real part of the other; and the imaginary part of one state with the imaginary part of the other. A purely imaginary matrix element will couple the real part of one state with the imaginary part of the other. This graph will truly be transitively connected only if the transition matrix elements are complex numbers with both real and imaginary parts. Otherwise the presence of a strongly regular drift matrix (which in time produces a rotation from real to imaginary space) can generate the "missing" elements of the Lie algebra, i.e., complete the transitivity of the Quantum Transfer Graph. These features of Quantum Transfer Graphs are shown in Fig. 1. Other modifications introduced in a recent paper[17] such as ordering the state in energy and the thickness of the edges representing the strength of the couplings are retained.

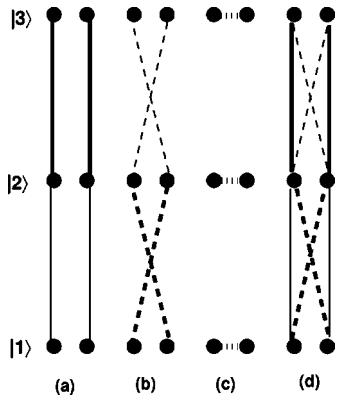

FIG. 1. Features of a Quantum Transfer Graph. Three nondegenerate eigenstates of the field-free Hamiltonian are represented by double nodes, representing the real (left) and imaginary (right) parts of the complex wave function. States that are transitively connected in the classical sense are not necessarily connected when the doublet structure is employed. A control matrix with $\imath$ times symmetric structure connects nodes as shown in (a). A control matrix with real, skew-symmetric structure connects nodes as shown in (b). The drift Hamiltonian causes rotations between the real and imaginary nodes of each eigenstate as in (c). The control matrix with a general complex, skew-Hermitian structure transitively connects the real *and* imaginary parts of the eigenstates as in (d).

IV. CONTROL IN THE INTERACTION PICTURE

In quantum physics, one often uses the interaction picture by making a unitary transformation that is very similar to transforming into the rotating frame in classical physics. Remembering that A is diagonal and $=\imath H_0$, this is carried out as follows:

$$Y = \exp(-At)X, \tag{12}$$

$$\dot{Y} = -A\exp(-At)X + \exp(-At)\dot{X} \tag{13}$$

$$= -A\exp(-At)X + \exp(-At)(A + \sum_i u_i(t)B_i)X \tag{14}$$

$$= \sum_i u_i(t)\exp(-At)B_iX \tag{15}$$

$$= \sum_i u_i(t)\exp(-At)B_i\exp(At)Y \tag{16}$$

$$= \sum_i u_i(t)\left[B_i + \frac{-t}{1!}[A,B_i] + \frac{(-t)^2}{2!}[A,[A,B_i]] + \cdots\right]Y \tag{17}$$

$$= \sum_i u_i(t)\tilde{B}_iY. \tag{18}$$

The transformed state vector Y evolves on an adjoint orbit of $U(n)$ with a span of $N(N-1)$. The last expansion (Baker–Campbell–Hausdorff expansion) contains the Lie algebra formed by the drift and control matrices. In the case that the system is controllable, these matrices span a space of dimension $N(N-1)$. Therefore, the presence of a strongly regular drift matrix, and a transitively

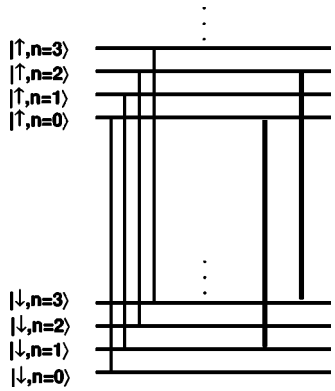

FIG. 2. Trapped-ion quantum states coupled by control fields with frequencies ω_c and ω_r. They cause transitions denoted by solid (carrier) and dashed (red sideband) lines, respectively. By changing the strength of the trap, it is possible to reduce one of the transition strengths to zero, thus truncating the infinitely large Hilbert space.

connected set of eigenstates is sufficient to show controllability. In exactly the same manner, if a set of eigenstates is transitively connected in the interaction picture, and the drift matrix is strongly regular, then these are sufficient conditions to establish controllability as well.

We note that if we have a control matrix that has both symmetric and skew-symmetric parts as in Fig. 1(d), we know that we can generate the $N(N-1)$ elements of the algebra. The Quantum Transfer Graph is transitively connected even without the consideration of the drift matrix. In such a case the demand for the strongly regular drift matrix can be relaxed, and controllability can be shown even with drift matrices that are not strongly regular.[12]

V. SPIN-$\frac{1}{2}$ PARTICLE COUPLED TO FINITE HARMONIC OSCILLATOR

We now apply controllability analysis to a quantum system that is one of the scalable paradigms of a future quantum computer. The system is also interesting from the viewpoint of control, because the control matrices contain both symmetric and skew-symmetric elements. Our analysis can be extended to other systems with sequentially connected eigenstates such as those in N-level STIRAP, and the control of Zeeman states.

In a recent paper,[17] we showed that under certain circumstances, the model of a spin-$\frac{1}{2}$ particle coupled to finite harmonic oscillator is a good representation of a trapped ion with two essential internal states. The spin-$\frac{1}{2}$ model represents a two-level atom with an energy splitting $\hbar\omega_0$, where the frequency $\omega_0/2\pi$ is in the several GHz range. The atomic levels are coupled to the motion of the ion in a harmonic trap.[18] These quantized vibrational energy levels are separated by a frequency $\omega_m/2\pi$ in the MHz range. The Hamiltonian of this system without a control field applied to it (in atomic units) is

$$H_0 = \omega_0 \frac{\sigma_z}{2} + \omega_m \hat{n}. \tag{19}$$

The Pauli operator σ describes the equivalent spin-$\frac{1}{2}$ system, and the operator $\hat{n}$ is the number operator of the quantized simple harmonic oscillator. The eigenstates of the field-free system are characterized by two quantum numbers S_z, and n. When a bichromatic field is applied that causes transitions between states $|\downarrow,n\rangle$ and $|\uparrow,n\rangle$ (carrier transitions), and between states $|\downarrow,n\rangle$ and $|\uparrow,n-1\rangle$ (red sideband transitions), the system is sequentially connected. An important parameter of this system is the Lamb–Dicke parameter η_m that describes the extent of the ion's motion compared to the wavelength of the applied electromagnetic field. It is possible to adjust the strength of the trap (thereby adjusting η_m) such that one of the transition couplings goes to zero, and the state space is truncated to N-levels as shown in Fig. 2.

In the case when the extent of the ion's motion is comparable to the wavelength of the applied field, a matrix element of the control Hamiltonian in the field-free eigenbasis in the interaction picture can be written as[17]

$$\langle S'n'|H_I'|Sn\rangle = \Omega(t)2\ \mathrm{Re}[\langle S'|\sigma_+|S\rangle \otimes \langle n'|\exp(\imath(\eta_m(a_m + a_m^\dagger)))|n\rangle]. \tag{20}$$

The harmonic oscillator part of this matrix element[18] is written as

$$\langle n'|\exp(\imath(\eta_m(a_m + a_m^\dagger)))|n\rangle = \exp(-\eta_m/2)\sqrt{\frac{n_<!}{n_>!}}(\imath\eta_m)^{|n'-n|}L_n^{|n'-n|}(\eta_m^2). \tag{21}$$

The symbol $n_>$ refers to the larger of n and n', and $n_<$ refers to the smaller of n and n'. $L_n^\alpha(x)$ is the associated Laguerre polynomial. When the applied field connects states $|\downarrow,n\rangle$ and $|\uparrow,n\rangle$ (carrier transitions), $n'=n$, and when the applied field connects states $|\downarrow,n\rangle$ and $|\uparrow,n-1\rangle$ (red sideband transitions), $n'=n-1$. The matrix elements are zero for all other values of n'. The strength of the ion trap can be adjusted (thereby adjusting η_m) so that the coupling strength of one of the (red or carrier) transitions becomes zero, the system is transformed into a finite closed subsystem, and a remaining infinite subsystem. For example, if the argument of the Laguerre polynomial η_m^2 is adjusted to 0.527 667 so that $L_6^1(\eta_m^2)=0$, the $|\downarrow,6\rangle$ to $|\uparrow,7\rangle$ transition is turned off.

The truncated finite system is now an N-level sequentially dipole coupled system. The electric field corresponding to the frequencies that cause the carrier and red transitions are dubbed E_c and E_r, respectively. The eigenstates can be ordered as $|\uparrow,0\rangle$, $|\downarrow,0\rangle$, $|\uparrow,1\rangle$, $|\downarrow,1\rangle,\ldots$. The drift Hamiltonian H_0 of this system can be written in matrix form as

$$\begin{pmatrix}
0 & 0 & 0 & 0 & 0 & 0 & \cdots & 0 & 0 \\
0 & \omega_0 & 0 & 0 & 0 & 0 & \cdots & 0 & 0 \\
0 & 0 & \omega_m & 0 & 0 & 0 & \cdots & 0 & 0 \\
0 & 0 & 0 & \omega_0+\omega_m & 0 & 0 & \cdots & 0 & 0 \\
0 & 0 & 0 & 0 & 2\omega_m & 0 & \cdots & 0 & 0 \\
0 & 0 & 0 & 0 & 0 & \omega_0+2\omega_m & \cdots & 0 & 0 \\
\vdots & \vdots & \vdots & \vdots & \vdots & \vdots & \ddots & & \\
0 & 0 & 0 & 0 & 0 & 0 & \cdots & \left(\frac{N}{2}-1\right)\omega_m & 0 \\
0 & 0 & 0 & 0 & 0 & 0 & \cdots & 0 & \omega_0+\left(\frac{N}{2}-1\right)\omega_m
\end{pmatrix}. \tag{22}$$

In the interaction picture, the Schrödinger equation is written as

$$\dot{Y} = (u(t)B_c + v(t)B_r)Y. \tag{23}$$

In general, we can assume that fields $E_c(t)$ and $E_r(t)$ do not have a phase difference between them. Then,

$$u(t) = c_1E_c(t) = 0.25\mu_0\exp(-\eta^2/2)E_c(t), \tag{24}$$

$$v(t) = c_2E_r(t) = 0.25\eta\mu_0\exp(-\eta^2/2)E_r(t), \tag{25}$$

$$B_c = \imath \begin{pmatrix} 0 & L_0(\eta^2) & 0 & 0 & 0 & 0 & \cdots \\ L_0(\eta^2) & 0 & 0 & 0 & 0 & 0 & \cdots \\ 0 & 0 & 0 & L_1(\eta^2) & 0 & 0 & \cdots \\ 0 & 0 & L_1(\eta^2) & 0 & 0 & 0 & \cdots \\ 0 & 0 & 0 & 0 & 0 & L_2(\eta^2) & \cdots \\ 0 & 0 & 0 & 0 & L_2(\eta^2) & 0 & \cdots \\ \vdots & \vdots & \vdots & \vdots & \vdots & \vdots & \ddots \end{pmatrix}. \tag{26}$$

$$B_r = \begin{pmatrix} 0 & 0 & 0 & 0 & 0 & 0 & \cdots \\ 0 & 0 & L_0^{(1)}(\eta^2) & 0 & 0 & 0 & \cdots \\ 0 & -L_0^{(1)}(\eta^2) & 0 & 0 & 0 & 0 & \cdots \\ 0 & 0 & 0 & 0 & L_1^{(1)}(\eta^2) & 0 & \cdots \\ 0 & 0 & 0 & -L_1^{(1)}(\eta^2) & 0 & 0 & \cdots \\ 0 & 0 & 0 & 0 & 0 & 0 & \cdots \\ 0 & 0 & 0 & 0 & 0 & -L_2^{(1)}(\eta^2) & \cdots \\ \vdots & \vdots & \vdots & \vdots & \vdots & \vdots & \ddots \end{pmatrix}. \tag{27}$$

The associated Laguerre polynomials $L_n^{\alpha}(x)$ can be written as

$$L_n^{\alpha}(x) = \sum_{k=0}^{n} (-1)^k \binom{n+\alpha}{n-k} \frac{x^k}{k!}. \tag{28}$$

The argument of the polynomials is the square of the Lamb–Dicke parameter η which gives a measure of how much the ion moves in the harmonic potential as compared to the wavelength of the light applied. We note that the control matrices for this system are different from the usual control matrices in quantum physics problems. The control matrix $\tilde{B}_c$ has the usual $\imath$ times symmetric structure. The control matrix $\tilde{B}_r$ has a real, skew-symmetric structure. If we take the Lie algebra formed by these two matrices, we get $N(N-1)/2$ independent matrices. As the drift matrix is strongly regular this system is completely controllable. We can further analyze this behavior in a four-dimensional model problem.

A. Example: A model four-dimensional system

Using a simple four-dimensional example,[2,19] we show how the Lie algebra produces successive elements, and spans the space. Consider a general matrix A for a four-dimensional Hilbert space with sequentially coupled eigenstates. In particular, we have

$$A = \begin{pmatrix} a & 0 & 0 & 0 \\ 0 & b & 0 & 0 \\ 0 & 0 & c & 0 \\ 0 & 0 & 0 & d \end{pmatrix}, \tag{29}$$

$$B_c = \imath \begin{pmatrix} 0 & \alpha & 0 & 0 \\ \alpha & 0 & 0 & 0 \\ 0 & 0 & 0 & \gamma \\ 0 & 0 & \gamma & 0 \end{pmatrix}, \tag{30}$$

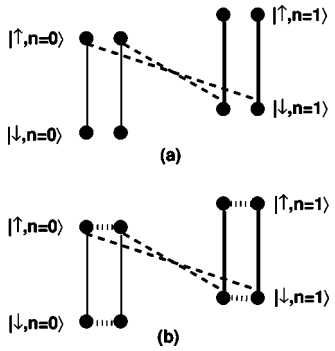

FIG. 3. Quantum Transfer Graph of a model four-level system. Control fields with frequencies ω_c and ω_r cause transitions denoted by solid (carrier) and dashed (red sideband) lines, respectively. The dotted lines in (b) demonstrate the effect of the drift Hamiltonian in rotating between the real and imaginary parts of each eigenfunction.

$$B_r = \begin{pmatrix} 0 & 0 & 0 & 0 \\ 0 & 0 & \beta & 0 \\ 0 & -\beta & 0 & 0 \\ 0 & 0 & 0 & 0 \end{pmatrix}. \tag{31}$$

Taking the Lie brackets of B_c and B_r, we produce four more linearly independent matrices $C=[B_c,B_r]/\beta$, $D=([B_c,C]-B_r*(\alpha^2+\gamma^2)/b)/(2\alpha\gamma)$, $E=[B_c,D]$, and $F=[E,B_r]/(-\beta)$. Thus the control matrices themselves produce $N(N-1)/2=6$ elements of the Lie algebra. Taking the Lie brackets of these six matrices with the drift matrix A, we get six more independent matrices with the opposite symmetry as the first six. Further Lie brackets of the two sets of six matrices produce the remaining four diagonal traceless matrices into which the strongly regular drift matrix can be decomposed.

B. Graphical analysis

We create a Quantum Transfer Graph to represent and analyze this system. We represent the various eigenstates $|\hat{S},n_m\rangle$ by double-vertices of a graph as shown in Fig. 3. When a resonant electromagnetic field is applied, the coupling between two eigenstates caused by the interaction form the edges. The eigenstates are ordered in energy, and the edges on the graph will represent the matrix elements of the interaction between the eigenstates (not a population flow between them), their thickness qualitatively indicating the strength of the coupling. The carrier field (with frequency ω_c) acting on an ion connects states $|\downarrow n\rangle$ and $|\uparrow n\rangle$. As the coupling matrix consists of real elements, this field connects the real parts to the real parts and the imaginary parts to the imaginary parts. The red sideband field (with frequency ω_r) connects states $|\downarrow n\rangle$ and $|\uparrow n-1\rangle$. Since the coupling matrix consists of imaginary elements, this field connects the real parts to the imaginary parts and vice versa. When both fields are applied simultaneously, we see that the Quantum Transfer Graph splits into two very interesting subgraphs. In the sense of the usual transfer graph,[4,20] all eigenstates are transitively connected. However, we can directly see the role of the drift Hamiltonian in moving this system from one subgraph to the other, and truly making the eigenstates transitively connected.

VI. SPECIFIC CONTROL SCHEME

We now discuss a specific control scheme for the *infinite* system, and show how the Quantum Transfer Graph helps us to describe the roles of the control and drift matrices in this scheme. In 1996, Law and Eberly[21] showed that by using the carrier and red fields *alternately* it is possible to produce arbitrary superpositions of a finite number of harmonic oscillator states. References 22 and 23 show that the same scheme can be used to generate arbitrary finite superposition states in

a spin-$\frac{1}{2}$/harmonic oscillator system. This scheme works by designing a sequence of alternately applied carrier and red sideband fields interspersed with a waiting time (action of the drift) in order to transfer the population from an arbitrary superposition to the ground state of the system $|\downarrow, n=0\rangle$. As seen by the Quantum Transfer Graph in Fig. 3(b), there are many combinations of the drift and control matrices that can be applied in order to get to the ground state (both in the finite and the infinite systems). The optimal combination will be one that time-optimizes the process subject to the constraint on the fields' intensities. This time-optimized Law–Eberly scheme is an interesting avenue for future work. Aspects of the controllability of the infinite-dimensional problem are discussed in related work by the authors.[24]

VII. CONCLUSION

A Quantum Transfer Graph is an effective tool in elucidating the controllability of finite quantum systems both in the Schrödinger and interaction pictures. We have shown the equivalence of sufficient conditions for controllability in both pictures, and explicitly presented the role of the drift matrix. We analyze the example of a sequentially connected N-level system as implemented by suitably designed quantum states of a trapped ion. Showing the mechanism of control, we explain how the specific Law–Eberly control scheme can be efficiently implemented.

ACKNOWLEDGMENTS

The authors thank Professor Roger Brockett (Harvard) and Professor M. Schlesinger (Windsor) for helpful comments. C.R. was supported by the Fellows program of the NSF Physics Frontiers Center at The University of Michigan, Ann Arbor. A.M.B. was supported by the National Science Foundation.

[1] M. Shapiro and P. Brumer, J. Chem. Phys. **84**, 4103 (1986).
[2] S. P. Shah, D. J. Tannor, and S. A. Rice, Phys. Rev. A **66**, 033405 (2002).
[3] V. Ramakrishna, M. V. Salapaka, M. Dahleh, H. Rabitz, and A. Pierce, Phys. Rev. A **51**, 960 (1995).
[4] G. Turinici, C. R. Acad. Sci., Ser. I: Math. **330**, 327 (2000); G. Turinici and H. Rabitz, Chem. Phys. **267**, 1 (2001).
[5] P. Zanardi and S. Lloyd, Phys. Rev. A **69**, 022313 (2004).
[6] N. Khaneja, R. Brockett, and S. J. Glaser, Phys. Rev. A **63**, 032308 (2001).
[7] J. M. Geremia, J. K. Stockton, and H. Mabuchi, Science **304**, 270 (2004).
[8] D. D'Alessandro, IEEE Trans. Autom. Control **47**, 87 (2002).
[9] A. M. Bloch, with J. Baillieul, P. E. Crouch, and J. E. Marsden, *Nonholonomic Mechanics and Control* (Springer-Verlag, New York, 2003).
[10] G. M. Huang, T. J. Tarn, and J. W. Clark, J. Math. Phys. **24**, 2608 (1983).
[11] R. W. Brockett, SIAM J. Control **10**, 265 (1972); SIAM (Soc. Ind. Appl. Math.) J. Appl. Math. **25**, 213 (1973).
[12] C. Altafini, J. Math. Phys. **43**, 2051 (2002).
[13] H. Fu, S. G. Schirmer, and A. I. Solomon, J. Phys. A **34**, 1679 (2001).
[14] N. V. Vitanov *et al.*, Adv. At., Mol., Opt. Phys. **46**, 57 (2001).
[15] J. P. Palao and R. Kosloff, Phys. Rev. Lett. **89**, 188301 (2002).
[16] A. R. P. Rau (private communication).
[17] C. Rangan, A. M. Bloch, C. Monroe, and P. H. Bucksbaum, Phys. Rev. Lett. **92**, 113004 (2004).
[18] D. J. Wineland *et al.*, J. Res. Natl. Inst. Stand. Technol. **103**, 259 (1998).
[19] A. R. P. Rau, Phys. Rev. A **61**, 032301 (2000).
[20] C. K. Law and J. H. Eberly, Opt. Express **2**, 368 (1998).
[21] C. K. Law and J. H. Eberly, Phys. Rev. Lett. **76**, 1055 (1996).
[22] B. Kneer and C. K. Law, Phys. Rev. A **57**, 2096 (1998).
[23] A. Ben-Kish *et al.*, Phys. Rev. Lett. **90**, 037902 (2003).
[24] R. W. Brockett, C. Rangan, and A. M. Bloch, Proceeding of the 42nd Conference on Decision and Control, Hawaii, December 2004, IEEE.